

## Environmental Effect on the Relative Contribution of the Charge-Transfer Mechanisms within a Short DNA Sequence

Heeyoung Kim and Eunji Sim\*

Department of Chemistry, Yonsei University, 134 Sinchondong Seodaemungu, Seoul 120-749, South Korea

Received: July 15, 2005; In Final Form: October 19, 2005

Time evolution of the charge-transfer site population is studied in a short DNA sequence to determine the type of governing charge-transfer mechanism. The system consists of a 5'-GAGGG-3' nucleobase sequence coupled with a dissipative bath that represents the DNA phosphate backbone and solvents. Relative contribution of transfer mechanisms to the whole charge-transfer process has been obtained using the on-the-fly filtered propagator functional path integral method with the density matrix decomposition. Partial density matrixes of the incoherent hopping and coherent superexchange pathways as well as the full reduced density matrix have been evaluated and discussed for both debye and ohmic baths. It was found that the relative contribution of the transfer mechanisms is rather sensitive to the frequency-dependent environmental description.

### 1. Introduction

Clear understanding of charge transfer in a duplex DNA is central to the development of bio- and nanotechnology. The charge transfer in a DNA double helix became important in molecular biology, as nucleobase oxidation is known to affect DNA damages and mutations.<sup>1</sup> Since Murphy et al. reported rapid photoinduced charge transfer over a 40 Å distance in DNA,<sup>2</sup> the potential application of DNA as a charge transport medium has drawn tremendous attention to molecular electronics, such as DNA-based functional nanoscale electronic devices which facilitate designing a nucleobase sequence as a molecular wire.<sup>3–5</sup> Although a large number of both theoretical and experimental studies have evolved in recent years, the mechanism for charge transfer in a duplex DNA still remains elusive. In general, the short-range DNA charge transfer has been explained as either of the two controversial mechanisms: It has been suggested that charges are localized on GC (guanine/cytosine) base pairs and transfer to distant GC base pairs by coherent superexchange through bridging AT (adenine/thymine) base pairs without ever residing on the bridge.<sup>6–9</sup> Alternately, it has been proposed that there is a noticeable contribution from incoherent hopping transport, either as a polaron-like hopping or as a true intermediate.<sup>10–13</sup> In particular, the latter has been supported by recent experiments, in which quantitative assessment of the distance dependence of charge-transfer efficiency has been shown to be incompatible to that of the exclusively coherent superexchange mechanism.<sup>11</sup> Furthermore, Zhang et al. have shown that the aqueous surroundings induce partial incoherence in an AT bridge base pair and cause the transfer mechanism to deviate substantially from the superexchange regime.<sup>13</sup>

In case that the substantial amount of charge accumulation is observed in the bridge state, the incoherent hopping mechanism is clearly confirmed. On the contrary, without a noticeable amount of charges accumulated in the bridge state, the transport mechanism remains elusive. Even if charges are, in fact, transported through incoherent hopping pathways, it may be

difficult to detect the population in a bridge state if the lifetime of the bridge state is much shorter than the characteristic time of the overall transport process. Furthermore, it is obvious that the superexchange transport does not allow charge accumulation in a bridge state. In practice, the experimental determination of the CT mechanism is performed in conjunction with the distance dependence. It is considered that the coherent superexchange rate constant decays exponentially with the distance between donor and acceptor, while the decrease of the incoherent hopping rate constant is rather insensitive to the distance change. Changing the molecular configuration by adding bridge units often creates another problem: the original energetic configuration of the short sequence is not maintained as the bridge length is changed. Furthermore, in the case that the transport dynamics of a single molecular configuration is available, the type of transport mechanism determined solely based on the transfer population is incomplete. Therefore, the quantitative analysis of the relative contribution of each transfer mechanism is necessary to support a conclusive argument.

If there exists an experimental setting that can measure the population of electrons that migrate through each pathway (without disturbing the other pathways), a consequent relaxation profile and intensity of each pathway can provide quantitative evidence of the relative contribution of the possible mechanisms. In this article, a relative contribution of a specific transport mechanism to charge transfer within a short DNA sequence is evaluated using the on-the-fly filtered propagator functional (OFPF) path integral method. To obtain the relative contributions of different types of mechanisms, path segments are separated to four types; incoherent hopping, coherent superexchange, partially coherent hopping, and static pathways in Hilbert space.<sup>14–16</sup> Charges hop from one site to its nearest neighbors by taking the incoherent hopping pathways while charges take a direct route between donor and acceptor in the coherent superexchange mechanism. The partially coherent hopping mechanism is also possible in which, within a single path segment, charges hop from donor (acceptor) to bridge and migrate directly between donor and acceptor. Although there is no contribution to the transport process, charges may not transfer from their initial state, hence the static paths. On the

\* To whom correspondence should be addressed. Fax: +82 2 365 7050. E-mail: esim@yonsei.ac.kr.

basis of the path separation, the reduced density matrix of the system is written as the sum of partial density matrixes of four mechanisms such that

$$\tilde{\rho}(t) = \tilde{\rho}^i(t) + \tilde{\rho}^c(t) + \tilde{\rho}^p(t) + \tilde{\rho}^s(t) \quad (1)$$

Superscript i stands for incoherent hopping, c for coherent superexchange, p for partially coherent hopping, and s for static pathways. Each pathway contributes to the full density matrix elements and is uncorrelated with other pathways, allowing independent computation of the path integration of the partial density matrix. If one of the mechanisms mostly governs the transport process, then contributions from other pathways can be ignored so that the full density matrix and the partial density matrix of the dominating mechanism become close. Thus, by computing  $\tilde{\rho}(t)$  and the partial density matrixes of interest, it is possible to determine the governing transport process as well as the relative and quantitative contribution of each mechanism.

The article is organized as follows: OFPF path integral formalism is discussed in section 2, and in section 3, the time evolution of the electronic population of a short DNA sequence is calculated in various environmental conditions. Both debye and ohmic environments are considered, and based on the numerical results, the relative contribution of the incoherent hopping and the coherent superexchange mechanism is discussed. Concluding remarks appear in section 4.

## 2. Methodology

Consider a charge (hole, radical cation) transport process between a GC single pair and a GC triple pair separated by an AT base pair in a DNA double helix form. After charge injection to the GC single pair, the charges migrate to the GC triple pair and are trapped. Although the charge migrates between the three electronic states, an important factor to the transport process is its surroundings, which consist of both the phosphate backbone and the solvent. By taking the three electronic states as the system of interest and the surroundings as the bath, the total Hamiltonian is written as

$$H = H_s(s) + H_b(\mathbf{x}) + H_{\text{int}}(s, \mathbf{x}) \quad (2)$$

Within a tight-binding system-bath Hamiltonian model, the system Hamiltonian  $H_s$  has the matrix representation in terms of three discrete oxidized electronic states that are involved in the charge transport; a donor (a GC base pair), a bridge (an AT base pair), and an acceptor (a triple GC base pair). The bare bath Hamiltonian  $H_b$  consists of an almost infinite number of harmonic oscillator modes, and weak bilinear interaction between the system and the bath is assumed within the linear response limit.

In practice, an infinite mode bath is used in terms of the spectral density  $J(\omega)$  instead of modeling a coupling constant of an individual mode. For a harmonic bath bilinearly coupled to the system, the spectral density is defined as a collection of the system–bath interaction in the frequency domain

$$J(\omega) = \frac{\pi}{2} \sum_j \frac{c_j^2}{m_j \omega_j} \delta(\omega - \omega_j) \quad (3)$$

The reorganization energy has the following relationship with the spectral density

$$\lambda = \frac{R^2}{\pi} \int_0^\infty d\omega \frac{J(\omega)}{\omega} \quad (4)$$

where  $R$  represents the distance between the two diabatic surfaces for which the reorganization energy is computed. For the donor–bridge–acceptor triad in this work, each diabatic surface is separated by equal distance of the unity and the donor–acceptor distance is two reduced units of distance.

Relaxation of the charge population of the three oxidized electronic sites in time is obtained from the reduced density matrix of the system defined as

$$\tilde{\rho}(t) = \text{Tr}_b[e^{-iHt/\hbar} \rho(0) e^{iHt/\hbar}] \quad (5)$$

where  $\rho(0)$  is the initial density matrix of the system and bath that are separable at thermal equilibrium. The trace of bath degrees of freedom results in a system exhibiting non-Markovian dynamics with nonlocal memory. For this reason, computation of the reduced density matrix is noniterative and the computation scales exponentially with time.

By the use of the OFPF path integral formalism,<sup>17</sup> partial density matrixes and the reduced density matrix in eqs 1 and 5 are converted into multidimensional path integrals in which each path is discretized in time with  $N$  time steps such that

$$\tilde{\rho}(s_N^\pm; t) = \sum_i \mathcal{T}(\Gamma_i; t - \Delta t) \cdot \mathcal{D}^e(\Gamma_i, s_N^\pm; t) \quad (6)$$

where the symbol  $s_k^+ = s^+(k\Delta t)$ ,  $\{k = 0, \dots, N\}$  denotes the coordinate at the time  $k\Delta t$  on the forward discretized path, while  $s_k^-$  corresponds to a coordinate on a path that runs in the backward time direction. In addition,  $\Gamma_i = \{(s_0^\pm)_i, (s_1^\pm)_i, \dots, (s_{N-1}^\pm)_i\}$  denotes the  $i$ th path survived that belongs to the mechanism of interest. The contribution of all possible paths that belong to the mechanism of interest should be taken into account. The history term  $\mathcal{T}$  involves interactions between the past time points

$$\begin{aligned} \mathcal{T}(\Gamma; t - \Delta t) = & \langle s_0^+ | \tilde{\rho}(0) | s_0^- \rangle \prod_{j=1}^{N-1} \langle s_j^+ | e^{-iH_s \Delta t / \hbar} | s_j^+ \rangle \langle s_j^- | e^{iH_s \Delta t / \hbar} | s_j^- \rangle \times \\ & \prod_{j=0}^{N-1} \prod_{j'=0}^j \exp \left\{ -\frac{1}{\hbar} [s_j^+ - s_j^-] [\eta_{jj'} s_{j'}^+ - \eta_{jj'}^* s_{j'}^-] \right\} \quad (7) \end{aligned}$$

while the propagator functional includes interactions between the present and the past time points in the form of

$$\begin{aligned} \mathcal{D}^e(\Gamma, s_N^\pm; t) = & \langle s_N^+ | e^{-iH_s \Delta t / \hbar} | s_N^+ \rangle \langle s_N^- | e^{iH_s \Delta t / \hbar} | s_N^- \rangle \\ & \times \prod_{j=0}^N \exp \left\{ -\frac{1}{\hbar} [s_N^+ - s_N^-] [\eta_{Nj} s_j^+ - \eta_{Nj}^* s_j^-] \right\} \quad (8) \end{aligned}$$

Expressions for the interaction coefficients  $\eta_{jj'}$  can be found in ref 18. Equation 6 terminates the propagation with the use of the endpoint propagator functional. During the actual simulation, the midpoint propagator, with the midpoint interaction coefficients, gives rise to an iterative propagation and is defined as

$$\begin{aligned} \mathcal{D}^m(\Gamma, s_j^\pm; t) = & \langle s_j^- | e^{iH_s \Delta t / \hbar} | s_j^- \rangle \\ & \times \prod_{j'=0}^j \exp \left\{ -\frac{1}{\hbar} [s_j^+ - s_j^-] [\eta_{jj'} s_{j'}^+ - \eta_{jj'}^* s_{j'}^-] \right\} \quad (9) \end{aligned}$$

The OFPF path integral approach effectively treats non-Markovian dynamics of a single-time reduced density matrix

as pseudo-Markovian dynamics of a multi-time augmented reduced density matrix by utilizing the finite time bath memory. Assuming the bath memory time spans  $N_\tau$  time steps, eq 6 is rewritten as

$$\tilde{\rho}(s_N^\pm; t) = \sum_i \mathcal{T}(\Gamma_i; t - \Delta t) \cdot \mathcal{L}^e(\Gamma_i, s_N^\pm; t) \quad N \leq N_\tau \quad (10)$$

$$\tilde{\rho}(s_N^\pm; t) \approx \sum_i \mathcal{T}(\Gamma'_i; t - \Delta t) \cdot \mathcal{L}^e(\Gamma'_i, s_N^\pm; t) \quad N > N_\tau \quad (11)$$

where  $\Gamma'_i = \{(s_{N-N_\tau+1}^\pm)_i, (s_{N-N_\tau+2}^\pm)_i, \dots, (s_{N-1}^\pm)_i\}$  includes only  $N_\tau$  time points. It is straightforward that although the number of paths to be integrated increases exponentially with time in eq 10, it no longer grows in eq 11. Therefore, the scaling of the computation ceases to increase by employing the pseudo-Markovian dynamics of a multi-time augmented reduced density matrix. Furthermore, the exponential increase of the number of paths in eq 10 can be tremendously decreased through on-the-fly filtering of the significant path segments. The final expression of eqs 10 and 11 becomes

$$\tilde{\rho}(s_N^\pm; t) = \sum_{w_i > \theta} \mathcal{T}(\Gamma_i; t - \Delta t) \cdot \mathcal{L}^e(\Gamma_i, s_N^\pm; t) \quad N \leq N_\tau \quad (12)$$

$$\tilde{\rho}(s_N^\pm; t) \approx \sum_{w_i > \theta} \mathcal{T}(\Gamma'_i; t - \Delta t) \cdot \mathcal{L}^e(\Gamma'_i, s_N^\pm; t) \quad N > N_\tau \quad (13)$$

where the summation includes only the paths with the weight bigger than the cutoff  $\theta$ . The weight is defined as  $w_i = |\mathcal{T}(\Gamma_i; t - \Delta t) \cdot \mathcal{L}^{e/m}(\Gamma_i, s_N^\pm; t)|$ . The weight cutoff is adjusted to provide desired numerical accuracy and is typically in the order of  $10^{-8}$  to  $10^{-10}$ .

### 3. Results and Discussion

By taking the ionization potential energy differences, the acceptor-state energy is 0.096 eV lower and the bridge-state energy is 0.47 eV higher than the donor-state energy.<sup>19,20</sup> The donor–bridge and bridge–acceptor electronic coupling constants are, however, still controversial in the literatures. According to Voityuk et al., the electronic coupling between neighboring bases differs with respect to nucleobase sequences.<sup>21</sup> On the other hand, others reported that the coupling constants between nucleobases are independent of the sequence.<sup>22,23</sup> In this work, we adapted the sequence-independent coupling constants between nucleobases as  $V_{GA} = V_{AG} = 0.025$  eV.<sup>22</sup>

It has been known that the type of governing charge-transfer mechanism is altered due to the energy difference between the donor and bridge while the incoherent hopping, coherent superexchange, and partially coherent hopping transfer mechanisms coexist for a wide range of the energy gap.<sup>16</sup> However, the charge-transfer mechanism is expected to be rather insensitive to the choice of electronic coupling constants; donor–bridge electronic coupling controls the decay of electronic accumulation in a donor state, and in contrast, the bridge–acceptor electronic coupling affects the charge accumulation in a bridge state in the course of an incoherent hopping transition.<sup>24</sup> In this article, we examine the effect of the environment. We use spectral density to describe the bath property, which is relevant to the dynamics of the system and also explore frequency-dependent environmental effects by comparing the influence of debye and ohmic spectral densities. Each electronic state is assumed to interact only with its nearest-neighbors, and the system is initially in the donor state. All simulations presented in this section have been performed at room temperature.

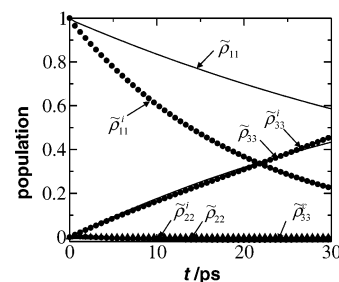


**Figure 1.** Time evolution of the charge accumulation on the three electronic sites coupled to the debye spectral density with the reorganization energy  $\lambda = 0.04$  eV. The debye frequency was chosen to be  $\omega_d = 0.1$  eV. Solid lines correspond to the full reduced density matrix for which all possible paths are taken into account while circles correspond to the partial density matrix of the incoherent hopping mechanism. The coherent superexchange contribution to the acceptor charge accumulation is also plotted as triangles but is negligible.

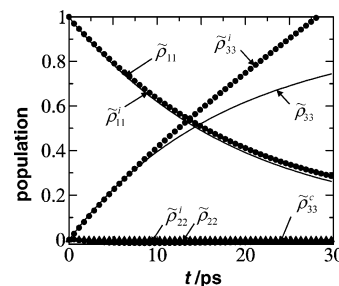


**Figure 2.** Same as Figure 1 with the reorganization energy  $\lambda = 0.16$  eV.

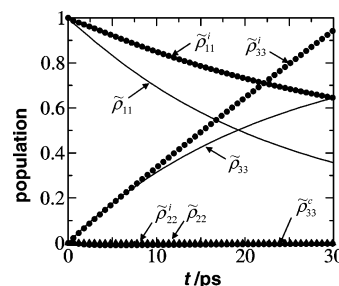


**Figure 3.** Same as Figure 1 with the reorganization energy  $\lambda = 0.31$  eV.

**A. Debye Spectral Density.** For a realistic description, polar solvent is often described in terms of the debye spectral density. The debye spectral density for DNA in water takes the following form<sup>25</sup>

$$J(\omega) = \frac{j_d \omega}{\omega^2 + \omega_d^2} \quad (14)$$

where  $\omega_d$  represents the debye frequency. Initially, the debye frequency is set to be 0.1 eV, which is close to the donor–acceptor energy gap. The effect of high-frequency modes is examined later in this section using spectral densities with  $\omega_d = 0.21$  eV.

Time evolution of the three diagonal elements of the reduced density matrix is shown in Figures 1–3 at various reorganization energies. The decay of the donor population over time represents the charge transfer to the bridge and acceptor while the rise of the acceptor population describes the charge accumulation due to charge trapping on the energetically favorable GC triple pair. The coherent superexchange pathway contribution to the rise of the acceptor population is also presented to be negligible, as is the charge accumulation on the AT bridge base pair. From

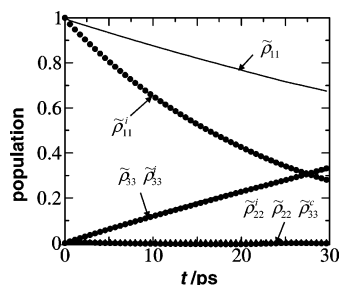


**Figure 4.** Same as Figure 1 with the debye frequency at  $\omega_d = 0.21$  eV.

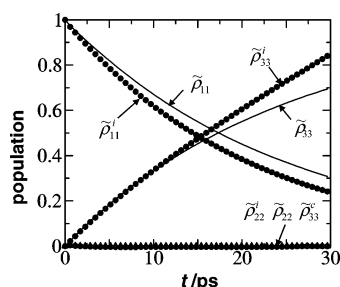


**Figure 5.** Same as Figure 4 with the reorganization energy  $\lambda = 0.16$  eV.

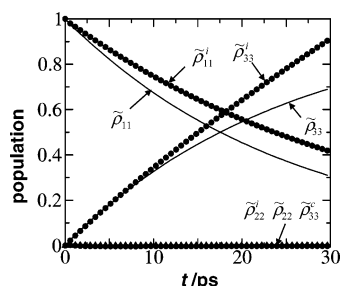


**Figure 6.** Same as Figure 4 with the reorganization energy  $\lambda = 0.31$  eV.

Figures 1–3, relative contributions of the incoherent hopping mechanism change with respect to the reorganization energy, as the reorganization energy alters the position of diabatic potential surface crossings.

With the low reorganization energy  $\lambda = 0.04$  eV in Figure 1, the incoherent hopping pathway contribution to the charge population in the donor state,  $\tilde{\rho}_{11}^i(t)$ , decays faster than  $\tilde{\rho}_{11}(t)$ . Note that each pathway either removes or accumulates charges in the donor state and that diagonal elements of the density matrix provide the net population change. Therefore,  $\tilde{\rho}_{11}^i(t) < \tilde{\rho}_{11}(t)$  indicates that the net effect of the incoherent hopping pathways on the donor-state population is to remove charges while the partially coherent hopping pathways redeposit charges in the donor states. As the reorganization energy becomes larger, the activation barrier height is lowered until the potential crossing reaches the activationless region. In other words, the superexchange transfer between donor and acceptor can occur easily since the activation energy is not required to cross surfaces. It is observed in Figure 2 that removing charges from the donor state through the incoherent hopping pathways is inhibited. As a result, it becomes favorable for partially coherent hopping pathways to transfer charges from donor to acceptor. Throughout Figures 1–3, it has been shown that the relative contribution and the role of each transfer mechanism vary with the bath reorganization energy within the debye environment.

Next, the effect of the high-frequency bath modes is examined using the debye frequency at  $\omega_d = 0.21$  eV. As observed in

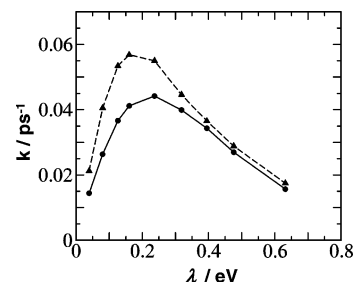


**Figure 7.** Charge-transfer rate constants as a function of the reorganization energy of the debye spectral density. Circles and triangles correspond to  $\omega_d = 0.21$  and  $0.1$  eV, respectively. The rate constants peaked near  $\lambda = 0.2$  eV and decrease with the reorganization energy. Lines between data points are drawn to guide the eye.

Figures 4–6, the transfer rate has been lowered compared to  $\omega_d = 0.1$  eV and bridge-state charge accumulation has not been observed. Without examining partial density matrixes, the bridge state with negligible population is often regarded as a virtual bridge of the coherent superexchange charge transfer. For the case of virtual bridges, it is practical to reduce the donor–bridge–acceptor triad model to a donor–acceptor two-level system in which a donor–acceptor coupling constant is effectively evaluated from donor–bridge and bridge–acceptor coupling constants. For instance, the McConnell product of the form, which depends on energy gap and electronic coupling constants between nearest-neighbor states, can provide an estimate of the effective superexchange coupling constant.<sup>26</sup> Upon evaluating the incoherent hopping partial density matrixes, however, it was found that the overall transition is controlled by the combination of the incoherent hopping and partially coherent hopping pathways. Use of the effective two-state model based on the insignificant bridge accumulation completely ignores the possibility of the incoherent hopping transport; therefore, for the short DNA sequence dealt with in this article, it is necessary to use the three-state model with an explicit bridge instead of a simple two-state system. Again, the change in the relative contribution of the two mechanisms is clearly visible in Figures 4–6. Charge-transfer rate constants of the two debye spectral densities discussed above are compared in Figure 7. The rate constants peaked near  $\lambda = 0.2$  eV, although the position is somewhat different for the two spectral densities. The qualitative nature of the relative contributions of the incoherent hopping and the partially coherent hopping mechanism exhibits similar behavior for both debye spectral densities.

Recently, Wan et al. reported characteristic transfer time constants of 5 and 75 ps in the case of a 3'-ETGG-5' ethidium-modified DNA sequence<sup>27</sup> and 9 and 65 ps for aminopurine-modified DNA sequences.<sup>28</sup> In addition, Zhang et al. obtained a time constant of 5 ps through a 5'-GTGGG-3' duplex in water and suggested that 5 ps may be a characteristic time scale for the short-range charge transfer in DNA.<sup>13</sup> In Figure 7, we observed time constants between 16 and 50 ps, which qualitatively agree with the others. Additionally, by using the debye spectral density with  $\omega_d = 0.21$  eV and  $\lambda = 0.47$  eV, the population ratio between the acceptor and the donor gives rise to  $P_{GGG}/P_G \sim 32$ , which agrees excellently with Giese's  $P_{GGG}/P_G = 30$  for the same sequence.<sup>29</sup> It is also interesting to note that the value of the reorganization energy is close to 0.4 eV and coincides with that of a previous report by Cramer et al.<sup>30</sup>

**B. Ohmic Spectral Density.** In this section, a dissipative medium described with the ohmic spectral density is coupled to a 5'-GAGGG-3' DNA sequence. The ohmic spectral density has an exponential cutoff so that the high-frequency modes are not as significant as the debye spectral density. The ohmic



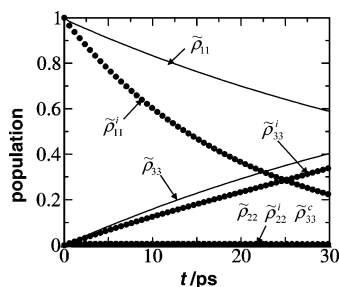


**Figure 8.** Same as Figure 4 with the ohmic spectral density with a cutoff frequency at  $\omega_c = 0.21$  eV.

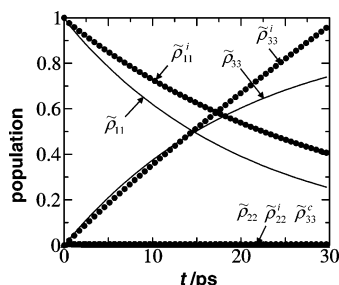


**Figure 9.** Same as Figure 8 with the reorganization energy  $\lambda = 0.16$  eV.

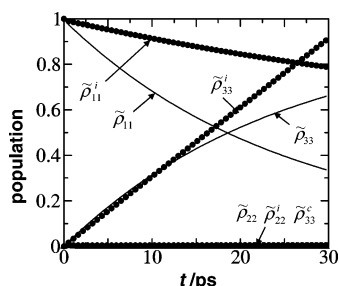


**Figure 10.** Same as Figure 8 with the reorganization energy  $\lambda = 0.31$  eV.

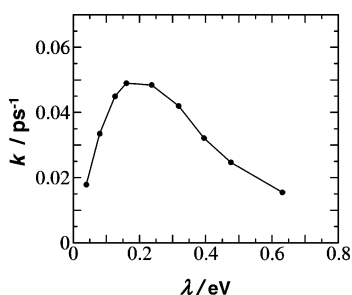


**Figure 11.** Charge-transfer rate constants as a function of the reorganization energy using the ohmic spectral density with the cutoff frequency  $\omega_c = 0.21$  eV. Lines between data points are drawn to guide the eye.

spectral density may represent nonpolar solvents as opposed to the debye spectral density which is usually considered to represent polar solvents.

The cutoff frequency of the ohmic spectral density was set to be 0.21 eV, to compare the results with the debye form discussed in the previous section. Figures 8–10 present the time evolution of the three-site populations and corresponding incoherent hopping contributions. Overall behavior is similar to the effect of the debye spectral density except for the position of potential crossings at a given reorganization energy. At  $\lambda = 0.16$  eV, in Figure 5 for the case of the debye environment, diabatic system potentials cross in the inverted region ( $\tilde{\rho}_{11}^i(t) < \tilde{\rho}_{11}(t)$ ), while corresponding potential crossings in the ohmic

environment occur in the normal region ( $\tilde{\rho}_{11}^i(t) > \tilde{\rho}_{11}(t)$ ) as shown in Figure 9.

Rate constants are also compared to represent the influence of high-frequency modes on the charge-transfer dynamics. The transfer rate constant of the system coupled to the ohmic environment with exponential cutoff is higher than that coupled to the debye environment, which shows a polynomial tail in the high-frequency limit. This is also consistent with what we observed in Figure 7: the system interacting with a low-frequency bath exhibits transfer that is more efficient than the one with the high-frequency mode emphasized bath. For a given short DNA sequence, stronger damping in the high-frequency bath modes results in slower dynamics in an overall transfer process.

To summarize this section, it was found that the environmental change affects the transfer mechanism, caused by the fluctuation in the potential surface crossing positions. It was observed that the relative contribution of transfer mechanisms is sensitive to the form of the spectral density. For this reason, the use of a frequency-dependent environmental description is important. Representation of the bath fluctuation with a single phenomenological parameter may produce an error in estimating the charge-transfer mechanism of the system of interest.

#### 4. Concluding Remarks

We investigated the charge transport mechanism in a short DNA sequence using the OFPF path integral method. By separating paths that belong to different mechanisms and by independently integrating contributions of each path, it was possible to determine the role of different pathways to the overall charge-transfer process. In general, the incoherent hopping pathways have been considered the most efficient and fastest transfer processes among the three transport types. In this article, for the given short DNA sequence, it was shown that a combination of the incoherent hopping and partially coherent hopping pathways led to the maximum transfer rate constant. Comparison between relaxations of the partial density matrixes provided comprehensive information on the analysis of the transport mechanisms. Within a short DNA sequence in which GC base pairs are separated by an AT base pair, it was found that both incoherent hopping and partially coherent hopping pathways contribute to the charge transport within closely stacked nucleobases such that incoherent as well as coherent migrations between states should be taken into account. In addition, the charge-transfer mechanism was influenced not only by the thermodynamic parameters of the system but also by the fluctuations due to the phosphate backbone and solvent. Therefore, the environmental effect should be considered in understanding the functions of DNA-based molecular electronic devices. In particular, to develop a feasible molecular wire, the long-range bridge-mediated CT mechanism in various DNA sequences, which is currently one of the most debated issues, should be known. Giese and co-workers have measured overall rate constants in a nucleotide sequence by varying the number of AT bridges.<sup>3</sup> The rate constants show dramatic changes as the number of bridges exceeds three AT base pairs. Giese et al. speculated that there is a significant mechanism change with the number of AT bridges. The methodology that we have used in this article is general for electron-transfer systems so that the extension for long sequences is straightforward. The system is modeled with an  $(n + 2) \times (n + 2)$  matrix where  $n$  denotes the number of AT bridge pairs. In fact, we are currently pursuing theoretical simulations to study the long-range CT mechanism in DNA sequences to quantify the relative contribution of each

CT mechanism to the overall transfer process. Although the computational difficulty increases exponentially with the size of the system, the pathway decomposed density matrix formalism will provide a quantitative basis for understanding the mechanism change in long-distance CT processes.

**Acknowledgment.** This work was supported by the Korea Science and Engineering Foundation (KOSEF) through Grant R04-2004-000-10009-0 and partly by Yonsei University. We thank Donghyun Kim for careful proofreading of the manuscript.

## References and Notes

- (1) Burrows, C. J.; Muller, J. G. *Chem. Rev.* **1998**, *98*, 1109.
- (2) Murphy, C. J.; Arkin, M. R.; Jenkins, Y.; Ghatila, N. D.; Bossman, S. H.; Turro, N. J.; Barton, J. K. *Science* **1993**, *262*, 1025.
- (3) Giese, B.; Amaudrut, J.; Köhler, A.-K.; Spormann, M.; Wessely, S. *Nature* **2001**, *412*, 318.
- (4) Fink, H.-W.; Schonenberger, C. *Nature* **1999**, *398*, 407.
- (5) Porath, D.; Bezryadin, A.; de Vries, S.; Dekker, C. *Nature* **2000**, *403*, 635.
- (6) Bixon, M.; Giese, B.; Wessely, R.; Langenbacher, T.; Michel-Beyerle, M. E.; Jortner, J. *Proc. Natl. Acad. Sci. U.S.A.* **1999**, *96*, 11713.
- (7) Berlin, Y. A.; Burin, A. L.; Ratner, M. A. *Chem. Phys.* **2002**, *275*, 61.
- (8) Brozema, F. C.; Berlin, Y. A.; Siebbeles, L. D. *J. Am. Chem. Soc.* **2000**, *122*, 10903.
- (9) Voityuk, A. A.; Rösch, N.; Bixon, M.; Jortner, J. *J. Phys. Chem. B* **2000**, *104*, 9740.
- (10) Henderson, P. T.; Jones, D.; Hampikian, G.; Kan, Y.; Schuster, G. B. *Proc. Natl. Acad. Sci. U.S.A.* **1999**, *96*, 8353.
- (11) Sartor, V.; Boone, E.; Schuster, G. B. *J. Phys. Chem. B* **2001**, *105*, 11057.
- (12) Conwell, E. M.; Rakhmanova, S. V. *Proc. Natl. Acad. Sci. U.S.A.* **2000**, *97*, 4556.
- (13) Zhang, H.; Li, X.-Q.; Hang, P.; Yu, X. Y.; Yan, Y. *J. Chem. Phys.* **2002**, *117*, 4578.
- (14) There is a relevant Liouville formalism by Mukamel and co-workers (Hu, Y.; Mukamel, S. *J. Chem. Phys.* **1989**, *91*, 6973) in which rate constants of the incoherent hopping and coherent superexchange transport are formulated by separating pathways in Liouville space. It should be noted that the pathways of Feynman's path integral formalism discussed in this article are defined in Hilbert space, that is, quantum mechanical trajectories in real-time and space.
- (15) Sim, E. *J. Phys. Chem. B* **2004**, *108*, 19093.
- (16) Sim, E. *J. Phys. Chem. B* **2005**, *109*, 11829.
- (17) Sim, E. *J. Chem. Phys.* **2001**, *115*, 4450.
- (18) Sim, E.; Makri, N. *Comput. Phys. Commun.* **1997**, *99*, 335.
- (19) Voityuk, A.; Jortner, J.; Bixon, M.; Rösch, N. *Chem. Phys. Lett.* **2000**, *324*, 430.
- (20) Bixon, M.; Jortner, J. *Chem. Phys.* **2002**, *281*, 393.
- (21) Voityuk, A. A.; Jortner, J.; Bixon, M.; Rösch, N. *J. Chem. Phys.* **2001**, *114*, 5614.
- (22) Troisi, A.; Orlandi, G. *Chem. Phys. Lett.* **2001**, *344*, 509.
- (23) Renger, T.; Marcus, R. A. *J. Phys. Chem. A* **2003**, *107*, 8404.
- (24) Sim, E.; Makri, N. *J. Phys. Chem. B* **1997**, *101*, 5446.
- (25) Yang, L.; Beard, W. A.; Wilson, S. H.; Broyde, S.; Schlick, T. *J. Mol. Biol.* **2002**, *317*, 651.
- (26) McConnell, H. M. *J. Chem. Phys.* **1961**, *35*, 508.
- (27) Wan, C.; Fiebig, T.; Kelley, S. O.; Treadway, C. R.; Barton, J. K.; Zewail, A. H. *Proc. Natl. Acad. Sci. U.S.A.* **1999**, *96*, 6014.
- (28) Wan, C.; Fiebig, T.; Schiemann, O.; Barton, J. K.; Zewail, A. H. *Proc. Natl. Acad. Sci. U.S.A.* **2000**, *97*, 14052.
- (29) Meggers, E.; Michel-Beyerle, M. E.; Giese, B. *J. Am. Chem. Soc.* **1998**, *120*, 12950.
- (30) Cramer, T.; Krapf, S.; Koslowski, T. *J. Phys. Chem. B* **2004**, *108*, 11812.